DOI: 10.1039/x0xx00000x

Article type: PAPER

Supporting Information

A Flexible Memory with Low-Voltage and High-Operation Speed Using an Al_2O_3/Poly(α-methylstyrene) Gate Stack on Muscovite Substrate

By Huixin He, † Waner He, † Jiaying Mai, Jiali Wang, Zhengmiao Zou, Dao Wang, Jiajun Feng, Aihua Zhang, Zhen Fan, Sujuan Wu, Min Zeng, Jinwei Gao, Guofu Zhou, Xubing Lu,* and J. -M. Liu

Mr. Huixin He, Miss. Waner He, Miss. Jiaying Mai, Miss. Jiali Wang, Mr. Zhengmiao Zou, Mr. Dao Wang, Prof. Zhen Fan, and Prof. Xubing Lu

Institute for Advanced Materials, South China Academy of Advanced Optoelectronics, and Guangdong Provincial Key Laboratory of Optical Information Materials and Technology, South China Normal University, Guangzhou, 510006, China
E-mail: luxubing@scnu.edu.cn (X. B. Lu)

Miss. Aihua Zhang, Prof. Sujuan Wu, Prof. Min Zeng, Prof. Jinwei Gao, and Prof. J. -M. Liu

Guangdong Provincial Laboratory of Quantum Engineering and Quantum Materials and Institute for Advanced Materials, South China Academy of Advanced Optoelectronics, South China Normal University, Guangzhou, 510006, China

Prof. Guofu Zhou

Guangdong Provincial Key Laboratory of Optical Information Materials and Technology and Institute of Electronic Paper Displays, South China Academy of Advanced Optoelectronics, South China Normal University, Guangzhou, 510006, China

Mr. Jiajun Feng and Prof. J. –M. Liu

Laboratory of Solid State Microstructures, Nanjing University and Innovation Center of Advanced Microstructures, Nanjing 210093, China

† These authors contributed equally to this work.

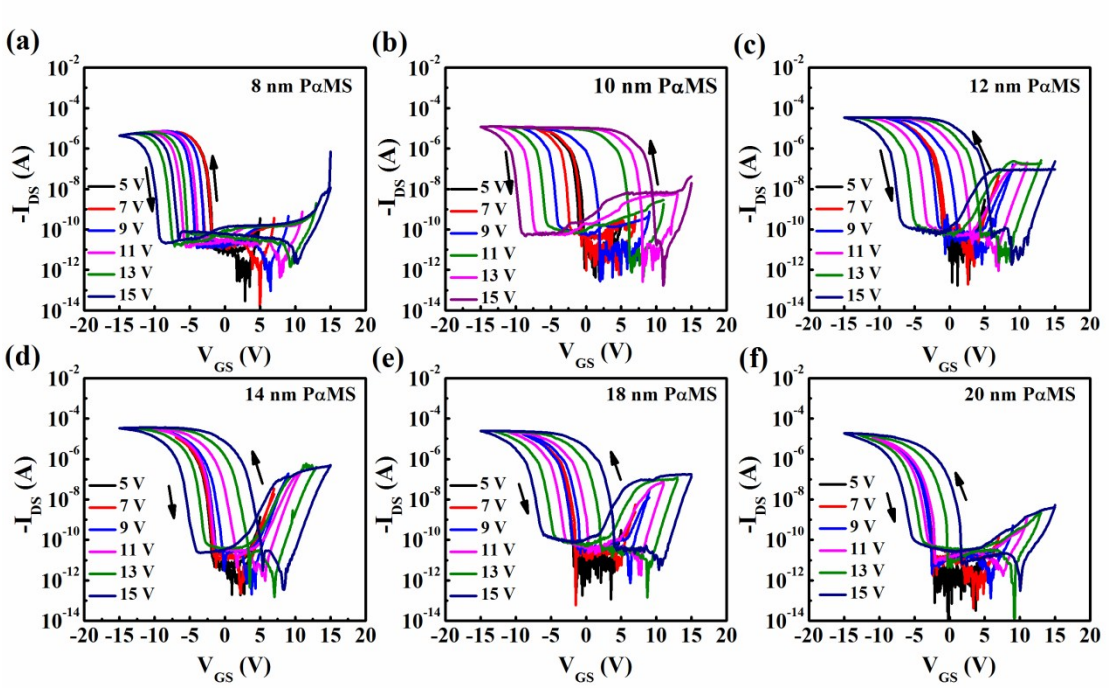

Fig. S1. Typical I_{DS}-V_{GS} characteristics for various V_{GS} sweeping ranges for OFET memory devices with various PαMS thicknesses: (a) 8 nm; (b) 10 nm; (c) 12 nm; (d) 14 nm; (e) 18 nm; (f) 20 nm. The Al_2O_3 is 20 nm thick and $V_{DS} = -3$ V.

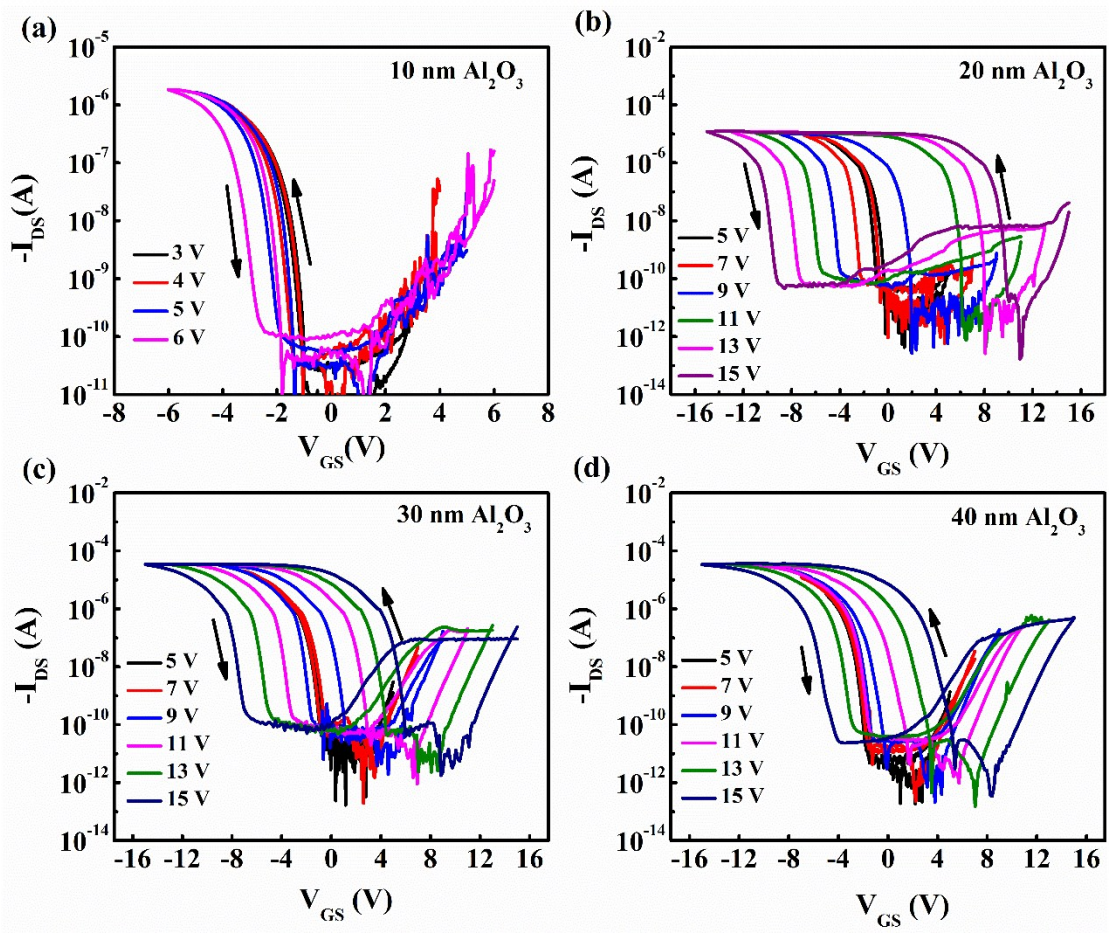

Fig. S2. Typical I_{DS}-V_{GS} characteristics at different V_{GS} sweeping ranges for OFET memory devices with various Al_2O_3 thicknesses: (a) 10 nm; (b) 20 nm; (c) 30 nm; (d) 40 nm. PαMS is 10 nm thick and $V_{DS} = -3$ V.

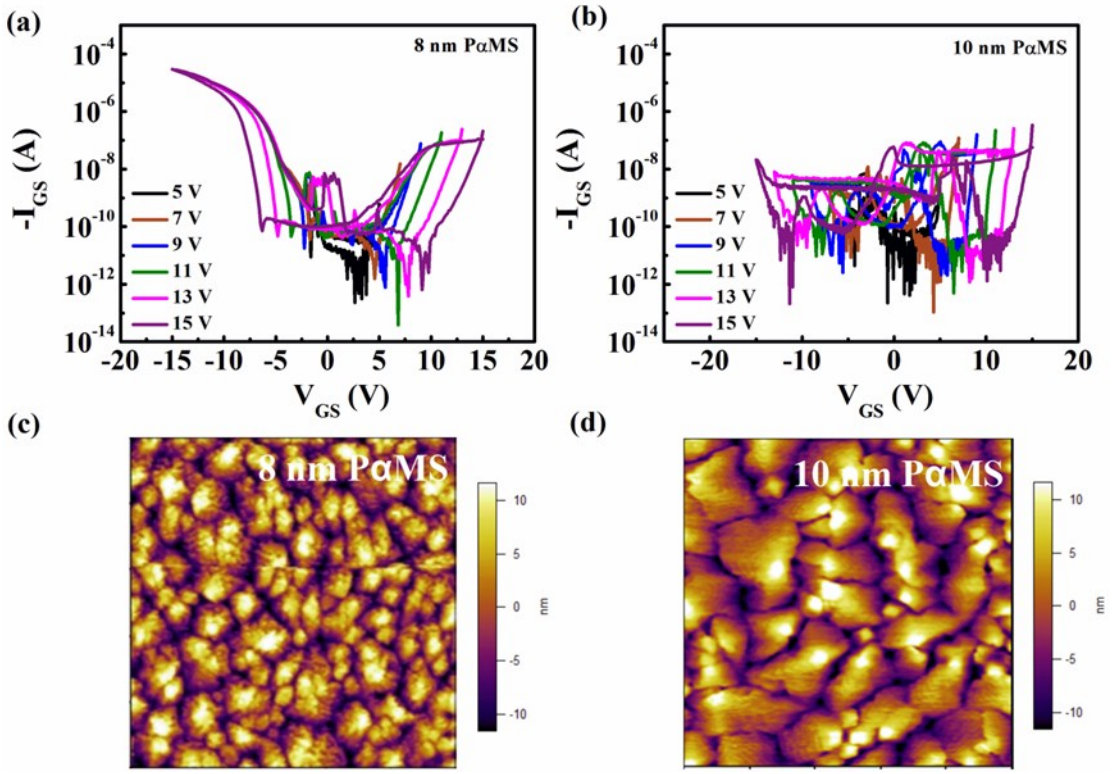

Fig. S3. Gate leakage current Characteristics of OFET memory devices with different thickness PαMS films: (a) 8 nm, (b) 10 nm. AFM surface topographies of pentacene film on different thickness PαMS films: (c) 8 nm, (d) 10 nm.

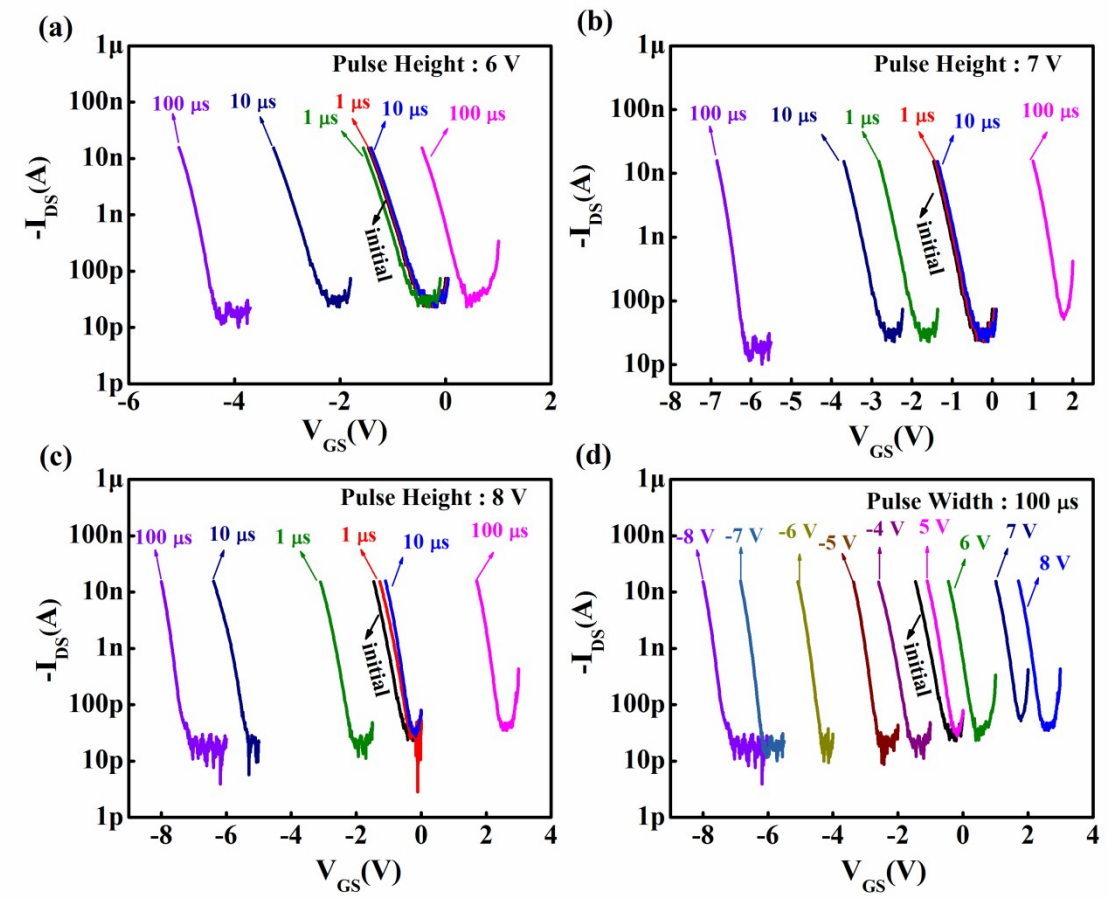

Fig. S4. Typical I_{DS}-V_{GS} curves for reading out V_{th} values for OFET memory with Al_2O_3(20 nm)/ PαMS (10 nm) gate stack: (a) pulse height is 6 V; (b) pulse height is 7 V; (c) pulse height is 8 V; (d) pulse width is 100 µs. $V_{DS} = -3$ V for all measurements.

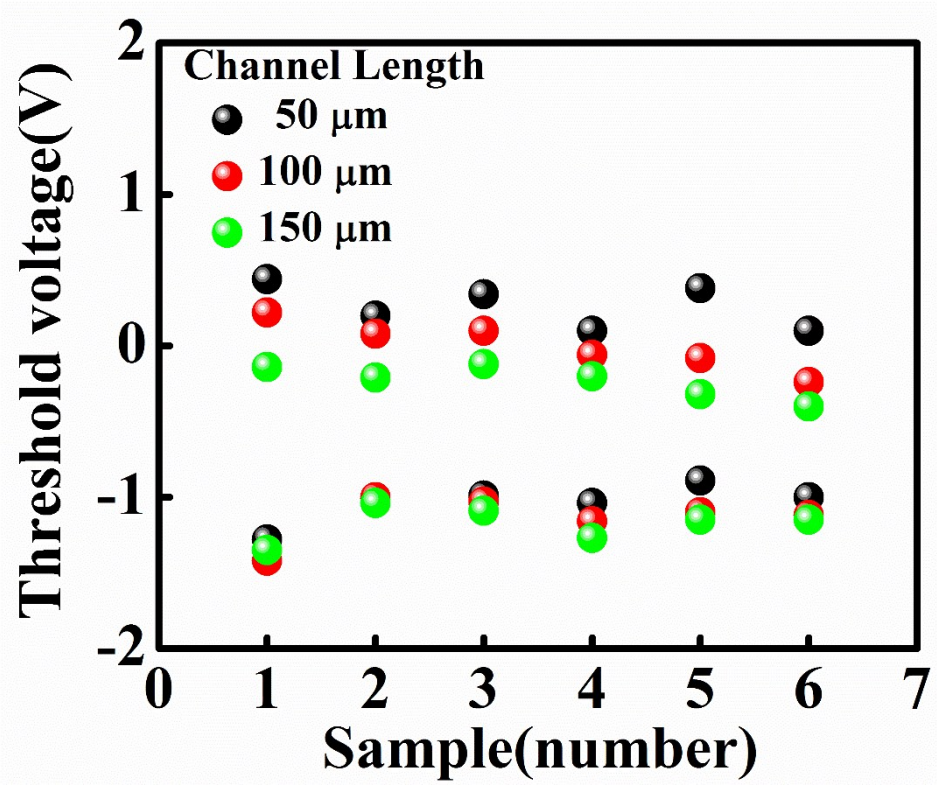

Fig. S5. V_{th} for various samples with different channel lengths after the +6 V, 100 μs program, −4 V, 100 μs erase. Each device has an Al_2O_3 (20 nm)/ PαMS (10 nm) gate stack.

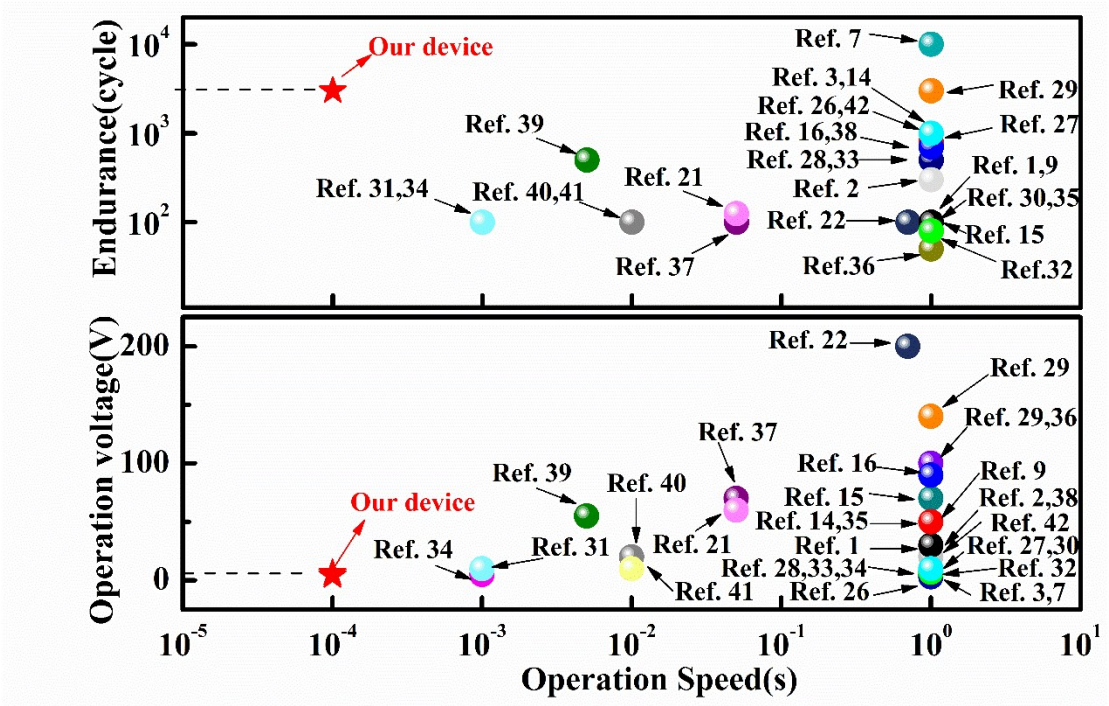

Fig. S6. Comprehensive comparison of operating voltage, operating speed, and endurance of proposed device with that of the representative flexible flash-type OTFT memory devices reported in recent years. The references here are from the main text.

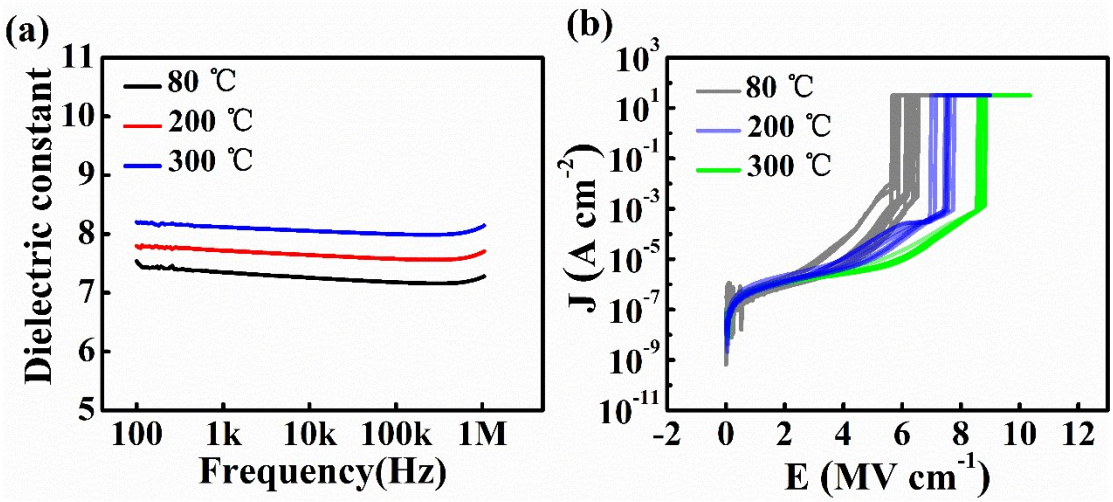

Fig. S7. Electrical properties of Al_2O_3 films fabricated at various temperatures. (a) Dielectric constant as a function of frequency. (b) Leakage current as a function of electric field.

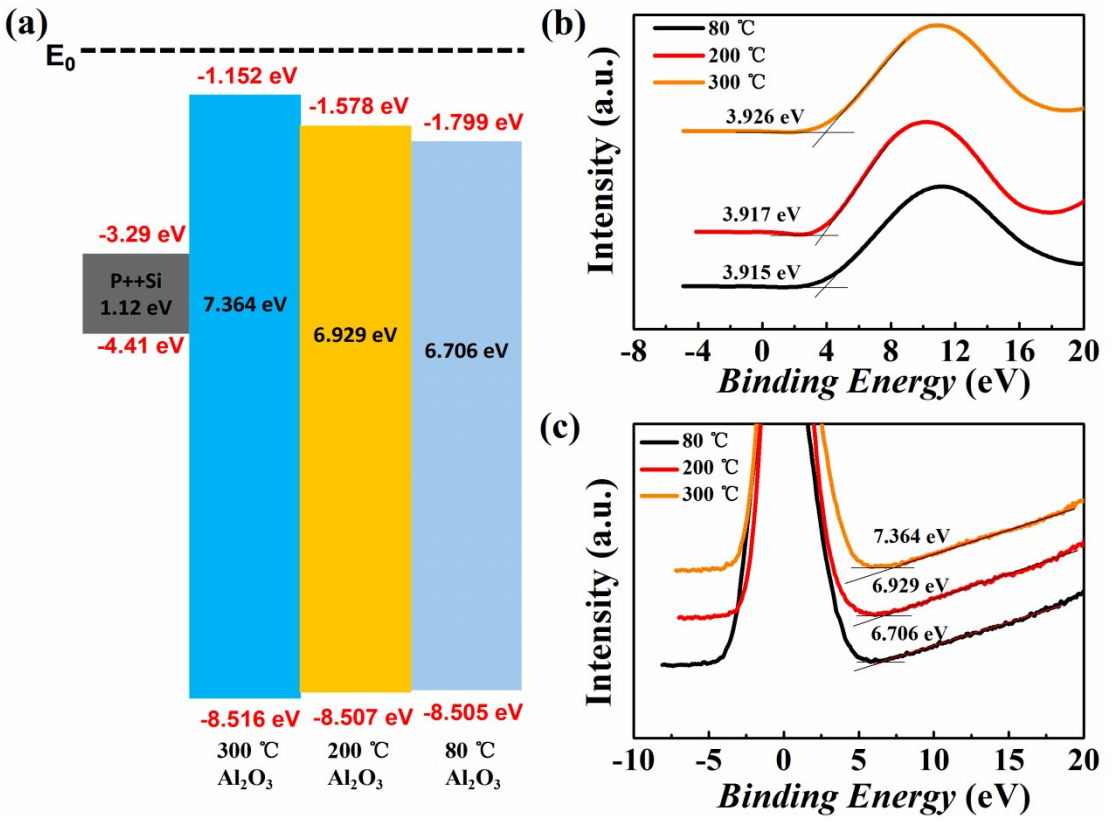

Fig. S8. (a) Band alignments of the Al_2O_3 dielectric with different deposition temperatures from the XPS;(b) XPS valence band spectra of Al_2O_3/Si with different deposition temperatures; (c) XPS O 1s electron energy loss spectra of Al_2O_3/Si with different deposition temperatures

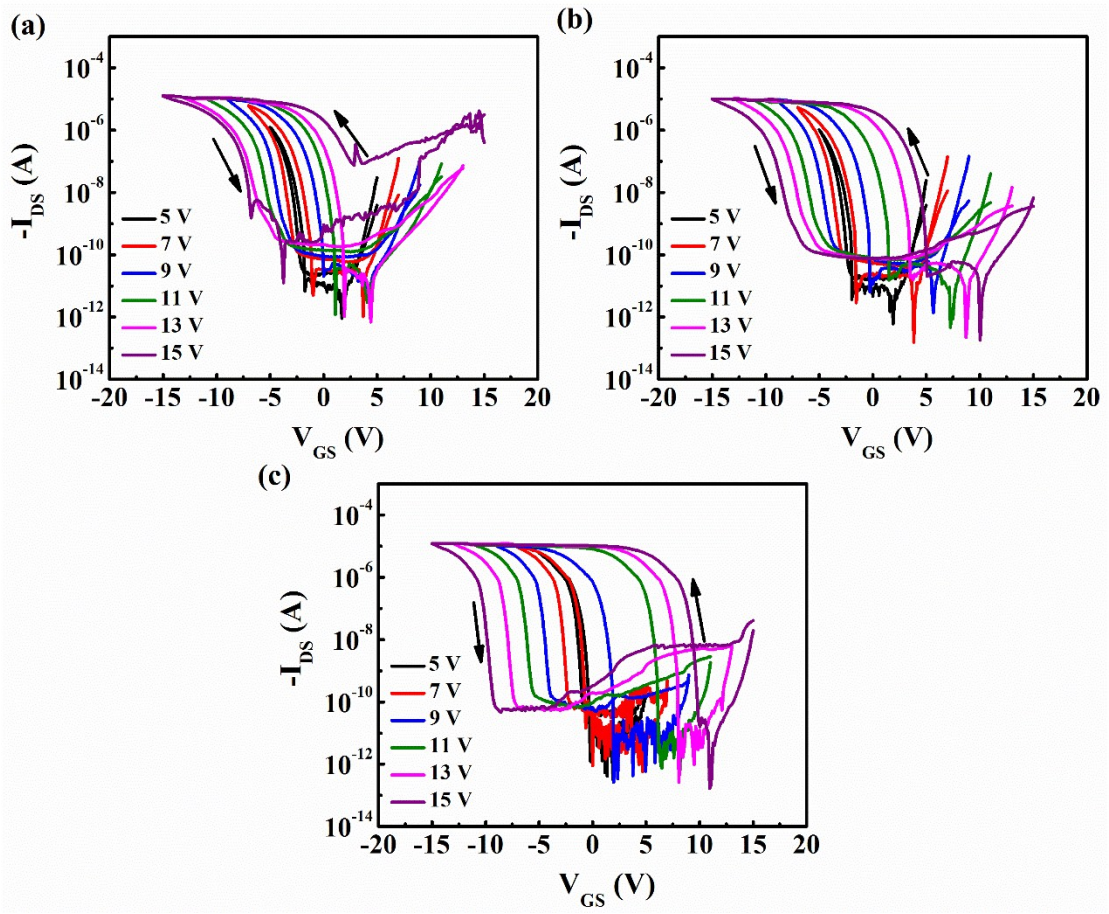

Fig. S9. I_{DS}-V_{GS} hysteresis characteristics of OFET memory devices with Al_2O_3 films fabricated at various temperatures: (a) 80 °C; (b) 200 °C; (c) 300 °C. The memory performance is lower for Al_2O_3 devices deposited at lower temperatures.

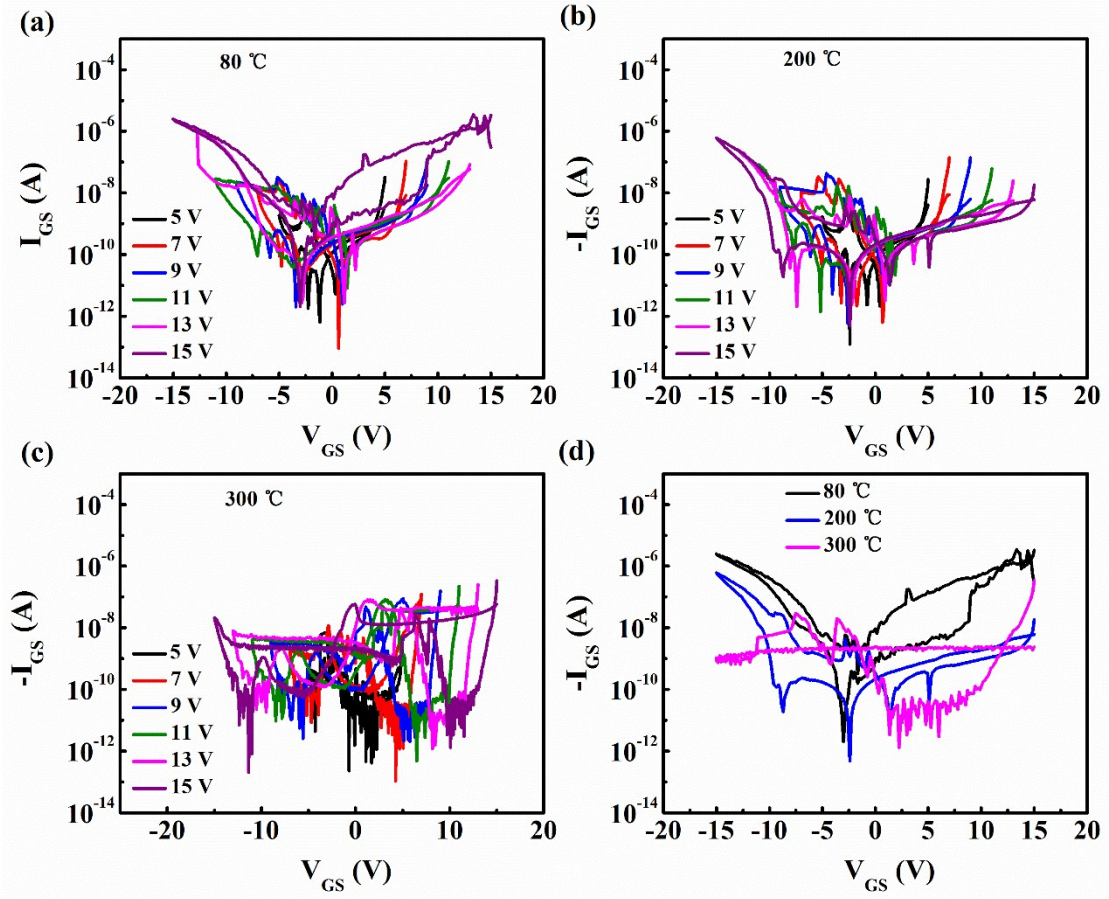

Fig. S10. Characteristics of gate leakage current of OFET memory devices with Al_2O_3 films fabricated at various temperatures: (a) 80 °C; (b) 200 °C; (c) 300 °C. (d) Comparison of gate leakage current during voltage scans between ±15 V. A higher gate leakage current occurs for Al_2O_3 devices deposited at lower temperatures.

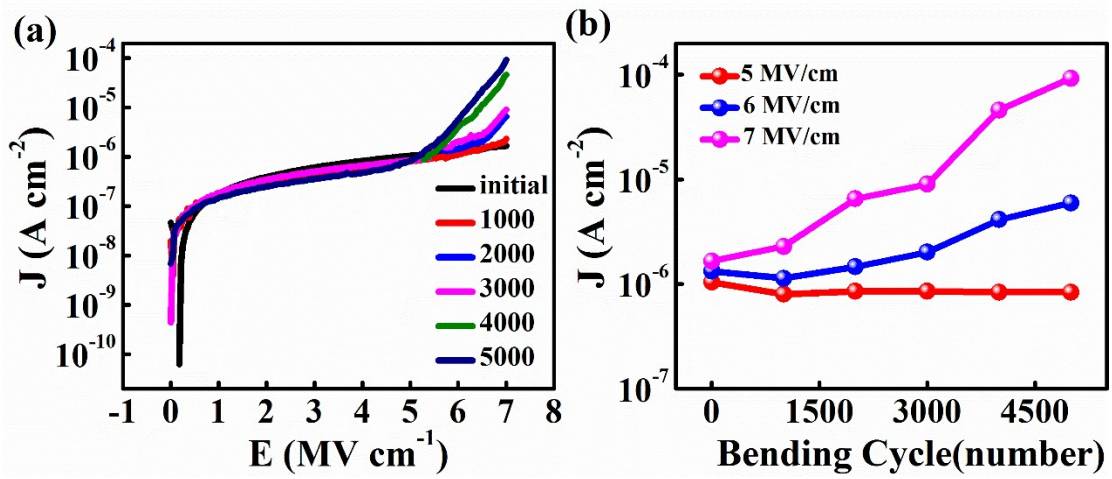

Fig. S11. Mechanical-bending properties of ALD-grown 20 nm Al_2O_3 film. (a) Leakage current as a function of electric field for Au/Al_2O_3/Au after various numbers of bending cycles at a fixed bending radius of 10 mm. (b) Leakage current density as a function of number of bending cycles with a bending radius of 10 mm and for various electric fields.

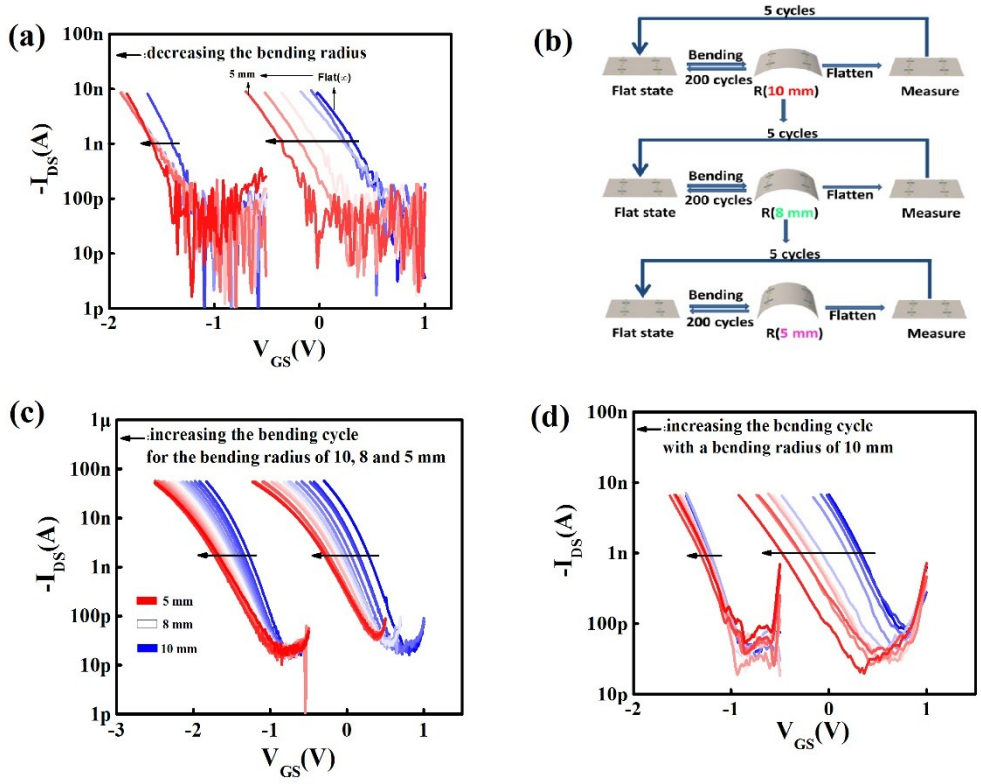

Fig. S12. Mechanical-bending properties of OFET memory device with PαMS (10 nm)/Al_2O_3 (20 nm) gate stack fabricated on a muscovite substrate. (a) Typical I_{DS}-V_{GS} curves for reading out V_{th} at various bending radii. (b) Schematic diagram of study of bending endurance with various bending radii. The threshold voltage was periodically recorded after a certain number of bending-unbending cycles. (c) Typical I_{DS}-V_{GS} curves for reading out V_{th} after various bending cycles with different bending radii. (d) Typical I_{DS}-V_{GS} curves for reading out V_{th} after various bending cycles at a fixed bending radius of 10 mm. All I_{DS}-V_{GS} curves were measured after the memory device was subjected to a +6 V, 100 μs program or a −4 V, 100 μs erase pulse at a V_{DS} = −3 V.